Neuron, Vol. 20, 619–624, April, 1998, Copyright ©1998 by Cell Press

Flash Decaging of Tyrosine Sidechains in an Ion Channel

Neurotechnique

Jeffrey C. Miller,*‡ Scott K. Silverman,†§ Pamela M. England,*† Dennis A. Dougherty,† and Henry A. Lester*‖
*Division of Biology
†Division of Chemistry and Chemical Engineering
California Institute of Technology
Pasadena, California 91125

Summary

A nonsense codon suppression technique was employed to incorporate *ortho*-nitrobenzyl tyrosine, "caged tyrosine," in place of tyrosine at any of three positions (93, 127, or 198) in the α subunit of the muscle nicotinic ACh receptor (nAChR) expressed in *Xenopus* oocytes. The *ortho*-nitrobenzyl group was then removed by 1 ms flashes at 300–350 nm to yield tyrosine itself while macroscopic currents were recorded during steady ACh exposure. Responses to multiple flashes showed (1) that each flash decages up to 17% of the tyrosines and (2) that two tyrosines must be decaged per receptor for a response. The conductance relaxations showed multiple kinetic components; rate constants ($<$0.1 s^{-1} to 10^3 s^{-1}) depended on pH and the site of incorporation, and relative amplitudes depended on the number of prior flashes. This method, which is potentially quite general, (1) provides a time-resolved assay for the behavior of a protein when a mutant sidechain is abruptly changed to the wild-type residue and (2) will also allow for selective decaging of sidechains that are candidates for covalent modification (such as phosphorylation) in specific proteins in intact cells.

Introduction

We introduce a technique for photochemically modifying a specific sidechain of an ion channel in an intact cell during electrophysiological investigation. Our goals are (1) to study the kinetics of gating processes at ion channels by devising a new type of time-resolved measurement, (2) to contribute to structure–function studies by measuring the approach to the wild-type conformation after a mutant sidechain is suddenly converted to the wild-type sidechain, and (3) to provide a tool for signal transduction research by monitoring function while abruptly and locally decaging sidechains that are candidates for subsequent covalent modification.

The method (Figure 1) employs the nonsense codon suppression technique for unnatural amino acid incorporation in *Xenopus* oocytes (Nowak et al., 1995, 1998; Saks et al., 1996). The unnatural amino acid contains a natural sidechain that is derivatized ("caged") by a photosensitive group. The photochemical strategy employs the well-characterized *ortho*-nitrobenzyl group (Lester and Nerbonne, 1982; Gurney and Lester, 1987; McCray and Trentham, 1989; Wieboldt et al., 1994; Nerbonne, 1996). Oocytes synthesize and incorporate into their membranes a channel in which such a caged sidechain occupies a selected position. Later, while the cell is under voltage-clamp study, a light flash photolyzes ("decages") the unnatural sidechain to produce the wild-type residue, apparently within 20 μs of photon absorption (Tatsu et al., 1996). We monitor the increased number of open channels as the receptor proteins relax from the less responsive mutant conformation(s) to the more responsive wild-type conformation(s).

Results

Analysis of Relaxation Amplitudes at nAChR α93 and α198

For the initial experiments, we investigated the nicotinic acetylcholine receptor (nAChR) of mouse muscle. We concentrated on two highly conserved and extensively studied tyrosine residues at positions 93 and 198 in the N-terminal extracellular region of the α subunit that are thought to participate in agonist binding (summarized by Galzi and Changeux, 1995; Karlin and Akabas, 1995; Nowak et al., 1995). For comparison, we also examined a less crucial tyrosine residue at position α127.

Figure 2 presents a typical experiment with an oocyte expressing Tyr(ONB) at position α93; similar results were obtained at α198. Figure 2A shows the raw traces from a chart recorder. At the start of the experiment, the membrane potential was held at −80 mV, and the holding current was small (−25 nA). The chamber was then perfused with ACh at 250 μM, a concentration ∼5-fold greater than the EC_{50} for the wild-type AChR. A small inward current (∼5 nA) was induced; this desensitized within ∼1 min. Then flashes were delivered at intervals of 20 s (in the illustrated example, we arranged for a longer interval of 80 s between the third and fourth flashes). The optical train was defocused from its optimal position, providing a lower flash intensity that clearly resolved the sigmoidal start (described below). The first 20 flashes are displayed. Each flash produced an abrupt increment of inward current (downward deflection). The subsequent slower upward deflection is desensitization, occurring with a time constant of ∼50 s, which is appropriate to this [ACh] at wild-type receptors (data not shown). The longer interval between the third and fourth flashes allowed for the observation that desensitization decreased the current resulting both from the immediately preceding flash and from all other previous flashes. In control experiments at α93 and at α198 (data not shown), no flash-induced increments were observed in the absence of ACh, but ACh applied after flashes then generated responses. There were no flash responses at wild-type receptors.

‡Present address: Department of Biology, Massachusetts Institute of Technology, Cambridge, Massachusetts 02139.
§Present address: Department of Chemistry and Biochemistry, University of Colorado at Boulder, Boulder, Colorado 80309.
‖To whom correspondence should be addressed.

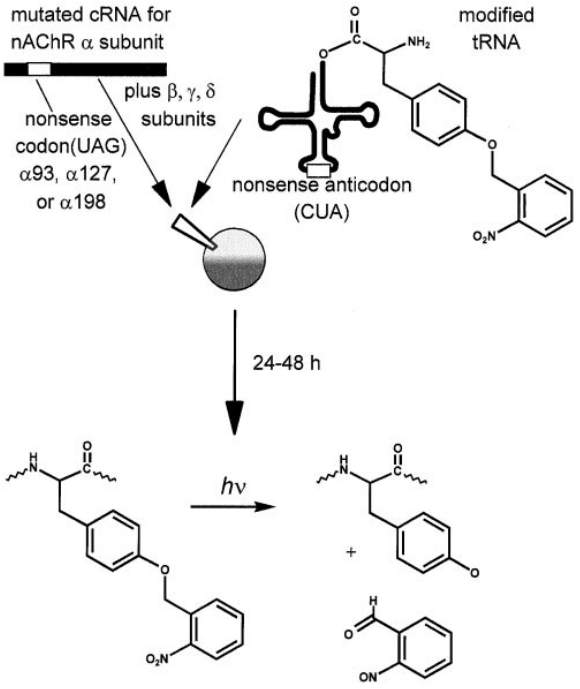

Figure 1. Schematic of the Method

In the top panel, an oocyte is injected with the mutated mRNA and the modified tRNA–Tyr(ONB). In the bottom panel, a Tyr(ONB) sidechain in an intact protein is photolyzed.

For the 20 flashes illustrated in Figure 2A, the flash-induced increments grew larger during the series. The increments for these flashes, as well as for the subsequent 50 flashes, are plotted in Figure 2B, which shows that the increment size then grew smaller after the first ~20 flashes.

Figure 2C, a cumulative plot of response amplitude versus flash number, conceptually reconstructs the total ACh-induced current in the imaginary absence of desensitization. This plot resembles a sigmoidal dose-response relation, and we have analyzed it according to standard dose-response principles. Thus, we assume (1) that each flash recruits an additional population of previously inactive receptors, which then respond to ACh and desensitize as in conventional experiments; and (2) that each receptor can be activated only after the photolysis of n caged sidechains. We also assume (3) that a constant fraction of remaining Tyr(ONB) residues is decaged with each flash. This fraction is conveniently expressed by analogy with a time-dependent process (Lester and Nerbonne, 1982). Thus, we fit the data in Figure 2C to the following equation:

$$I = I_{max}[f_0 + (1-f_0)(1-e^{-k_f t_f})]^n, \quad (1)$$

where k_f is the photolysis per flash and t_f is the total number of flashes. The parameter f_0 accounts for the small basal activity before illumination (6 nA, or ~0.3% of the maximal current, in the experiment of Figure 2). For positions α93 and α198, we assume that f_0 represents photolysis by stray light during the organic synthesis, microinjection, or biosynthesis steps before the light-flash experiment.

The data of Figure 2C fit well to Equation 1, yielding a value of $k_f = 0.048$/flash; that is, nearly 4.8% of the caged α93 sidechains are decaged in any one flash. We find that $n = 1.8$, so that nearly two caged Tyr sidechains must be photolyzed to activate each receptor. A value of $f_0 = 0.05$ accounts for the small response before any flashes occur.

Very similar values for k_f, n, and f_0 were obtained when Tyr(ONB) was incorporated at the α198 position; in pooled data from seven experiments at α93 and α198, the values for n ranged between 1.48 and 1.84. Any deviation from uniform flash intensity would decrease the experimental value of n from the expected value of two. With maximally focused optics, k_f ranged between 0.11 and 0.17/flash. We have also used a continuous 500 W Hg–Xe lamp as a light source; in this case, $k_f t_f$ becomes kt, and we estimate that $k = 0.7$/s.

At α93 and α198, analysis of flash-induced increments

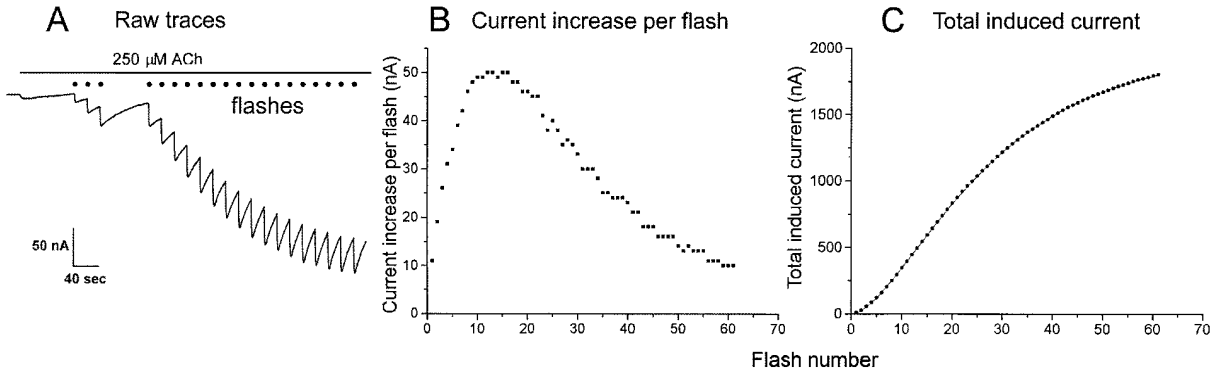

Figure 2. Analysis of the Conductance Increases that Occur When α93-Tyr(ONB) Receptors Are Exposed to ACh and to Light Flashes

(A) Raw traces from a chart recorder during decaging. The membrane potential was held at −80 mV. At the start of the experiment, the chamber was perfused with 250 μM ACh. A series of flashes was delivered at intervals of 20 s (with a longer interval of 80 s between the third and fourth flashes). The first 20 flashes are displayed. Each flash produces an increment of inward current, which then desensitizes.

(B) Increments for the first 70 flashes. The increment size peaks after 10–20 flashes.

(C) Cumulative plot of response amplitude versus flash number. The data are fit to equation (1), with $k_f = 0.048$/flash and $n = 1.8$.

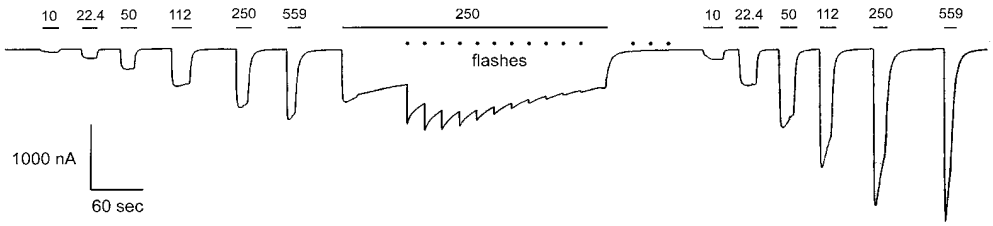

Figure 3. Responses to ACh before, during, and after Flashes at α127-Tyr(ONB) Receptors
The bars show perfusion of ACh at the indicated concentrations (μM).

thus confirms two major expectations for decaging a crucial sidechain in the nAChR α subunit. There is a clear requirement for two decaging events, which presumably correspond to the two α subunits in each nAChR, and desensitization occurs after activation.

At α127, There Is Activation before Photolysis

While receptors with Tyr(ONB) incorporated at either α93 or α198 responded similarly to decaging, a different pattern of responses was observed when Tyr(ONB) was incorporated at α127 (Figure 3). Appreciable ACh-induced currents were measured before photolysis; these responses had an EC_{50} value of 100–130 μM. Irradiation increased the currents by roughly 2-fold and decreased the EC_{50} to the wild-type value of ~50 μM. It appears that the nAChR with Tyr(ONB) incorporated at α127 is partially sensitive to ACh.

Bungarotoxin Effects

To test whether receptors with caged tyrosines at α93, α198, or α127 could bind α-bungarotoxin, we incubated oocytes expressing Tyr(ONB) at each of these positions in 125 nM α-bungarotoxin for 30–60 min, followed by a 5 min wash. When these oocytes were irradiated in the presence of ACh, their responses were decreased by >80% relative to control oocytes. Therefore the caged receptors, like wild-type receptors, are able to bind α-bungarotoxin. In additional experiments, 250 nM α-bungarotoxin was perfused with 50 μM ACh (which causes little desensitization) while light flashes were delivered to oocytes expressing either α93 or α127 Tyr(ONB) receptors. Flash-induced relaxation amplitudes decreased at least as rapidly as the steady ACh-induced currents, showing that the toxin blocked the caged receptors at least as rapidly as it blocked wild-type receptors. These data indicate that the caged receptors have overall structures that are similar to wild-type receptors.

The Conductance Increases Consist of at Least Two Phases

Figure 4 displays kinetic analyses of light-flash relaxations for Tyr(ONB) incorporated at each of the three positions, α93, α198, and α127. Strikingly, the relaxations cover a wide range of time scales, with at least two phases in each case. The more rapid phase, which we term phase 1, occurs with a time constant of 1–3 ms. Under the conditions of our experiments, this phase seems to be limited by the time course of the flash itself.

The slower phase, which we term phase 2, can be resolved in most of our experiments. At pH 7.0, phase 2 has a rate constant of 0.98 ± 0.1 s^{-1} at α93, 12.9 ± 1.6 s^{-1} at α198, and 52 ± 10 s^{-1} at α127.

In 10 oocytes subjected to flash series (five with α93 and five with α198), the fraction of the current increment due to phase 1 increased with flash number. For the first flash, phase 1 accounted for <10% of the total current increment. After 25 flashes, phase 1 accounted for 30%–80% of the current increment. The fractional contribution of phase 1 was also sensitive to experimental conditions such as [ACh] and flash frequency. The relaxations at α127 were too rapid for a systematic study of relative amplitudes.

The rate constant for phase 2 did not vary markedly (<20%) during any series of flashes. Also, the rate constant for phase 2 depended little (<15%) on [ACh] in the range from 10–250 μM or on membrane potential in the range −60 to −120 mV (data not shown).

The Rate Constants for the Slower Phase Depend on pH

Because the breakdown of the *aci*-nitro intermediate in *ortho*-nitrobenzyl photolysis is catalyzed by protons (McCray and Trentham, 1989), we studied the effect of pH on the relaxation rates (Figure 4, lower panels). Despite the nearly 10-fold greater rate constants for phase 2 relaxations at position α198 relative to α93, the two receptors displayed qualitatively similar rate increases with increasing pH. At α93, the rate constant increased from 0.086 ± 0.015 s^{-1} at pH 5.0 to 16 ± 0.2 s^{-1} at pH 9.0. At α198, the rate constants increased from 1.10 ± 0.03 s^{-1} at pH 5.0 to 24.6 ± 0.5 s^{-1} at pH 8.0. When these pH dependences were fit to a model with a single ionizable site, we obtained pK_a values of 6.6–7.1 for both receptors. Rate constants for α198 decreased moderately with further increases in pH, to 5.3 ± 0.3 s^{-1} at pH 9.0, suggesting that an additional process affects relaxations at higher pH.

On the other hand, α127-Tyr(ONB) displayed both faster phase 2 relaxations and increasing rates at lower pH (Figure 4). Also at α127, an additional, faster relaxation component appeared at high pH (Figure 4). The rate constant for this component decreased from 34 s^{-1} at pH 8.0 to 13 s^{-1} at pH 9.0.

Discussion

The present experiments show that in vivo sidechain decaging generates useful data by combining site-

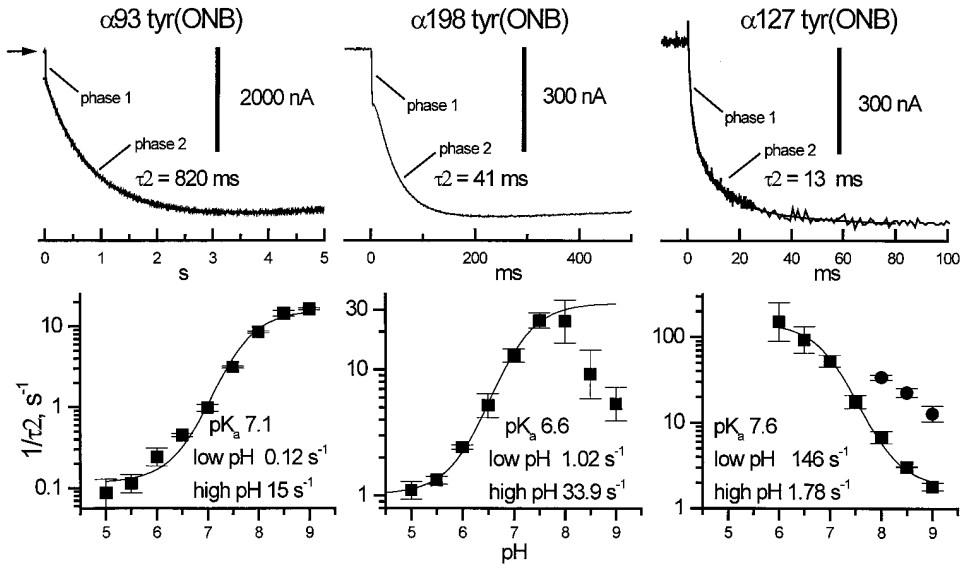

Figure 4. Kinetics of Light-Flash Relaxations for Each of the Three Positions Studied

The top panels show each relaxation on an appropriate time scale. [ACh], 250 μM; pH, 7.0, 7.5, and 7.0 for α93, α198, and α127, respectively. The arrow shows the baseline current before the flash (which occurs at time zero). Each relaxation begins with a rapid phase that appears instantaneous in the traces; this is phase 1. The slower phase (phase 2) is resolved and has a distinct time constant for each position. An exponential time course is superimposed on phase 2 for each trace. The optics were optimally focused, providing flash intensities almost 3-fold greater than those in the experiment of Figure 2. The lower panels show the pH dependence of rate constants for phase 2 at each of the three positions studied. The data were fit to a model with a single ionizable site, with pK_a, low pH limit, and high pH limit as indicated. Note that an additional faster relaxation component was present at high pH for α127; this was not fit to a titration curve.

directed mutagenesis and kinetic analysis on ion channels expressed in *Xenopus* oocytes. Individual flashes produce increases in ACh-induced current, and we can resolve these increases on the millisecond time scale. The conductance increments can be understood in terms of the classical finding that the channel opens only when both nAChR α subunits bind agonist.

The technique as presently implemented should also be effective in photolyzing intracellular caged sidechains, as previous work has demonstrated that a related nitrobenzyl cleavage (SNIPP) is efficient for intracellular residues (England et al., 1997). Although the technique is applied here to ion channels, it is expected to be applicable to any protein expressed in the oocyte system. Therefore, a phosphorylation site can be rapidly revealed by decaging a tyrosine, serine (Cook et al., 1995), or threonine sidechain. This capability will enable detailed studies on the timing and function of phosphorylation at specific residues with good spatial localization. It is also possible to cage carboxyl (Mendel et al., 1991) and, presumably, thiol and amino sidechains. In preliminary experiments, we have successfully incorporated 4,5-dimethoxy-*ortho*-nitrobenzyl tyrosine (nitroveratryl tyrosine), which is photolyzed at longer wavelengths and more efficiently than the *ortho*-nitrobenzyl derivative used here. Finally, the method would be even more useful if it could be generalized to mammalian cells.

Mechanistic Interpretation of the Relaxations

Interestingly, the relaxations initiated by decaging sidechains at the nAChR cover a wide range of time scales. Phase 1 is too fast to be well resolved under our present conditions (room temperature and rather high [ACh]), but one expects a relaxation on this time scale from wild-type receptors subjected to a sudden jump of agonist concentration or voltage (Adams, 1981; Figl et al., 1996). We therefore tentatively assign phase 1 to a process much like that of normal physiological activation. Assuming that receptors must attain the wild-type closed conformation before opening, we conclude that some receptors do so within 3 ms after photolysis, either (1) because some receptors with caged sidechains already have the correct conformation, even though the *ortho*-nitrobenzyl group at α93 or α198 might partially prevent agonist binding (Galzi and Changeux, 1995; Nowak et al., 1995); or (2) because some decaged receptors rapidly undergo a transition from an inappropriate closed conformation to the wild-type closed conformation.

Phase 2 is up to 10^4-fold slower than phase 1—the phase 2 time constant exceeds 11 s at low pH for α93. The major pH dependence of the phase 2 rates at α198 and at α93 is opposite to the trend expected if this phase is governed by the breakdown of an intermediate in the dark reaction following photon absorption. In addition, the absolute rates are several orders of magnitude slower than the expected dark reaction rates (McCray and Trentham, 1989). Phase 2 for the α198 and α93 mutants could therefore correspond to a conformational change with a substantial energy barrier for some of the receptors upon decaging. In contrast, phase 2 is more rapid at α127, and it has a pH dependence appropriate to the dark reaction for photolysis (McCray and Trentham, 1989). Therefore, it is possible that the dark reaction governs phase 2 for the α127-Tyr(ONB) mutant, indicating that the local environment within the protein can

decrease the rate of the photolysis relative to the measurements in free solution (McCray and Trentham, 1989; Tatsu et al., 1996).

If phase 2 in α93 and α198 mutant receptors is indeed caused by a conformational change, this transition evidently has a strongly pH-dependent rate constant, with an apparent pK_a of 6.6–7.1. Of the natural sidechains, only histidine has a pK_a near this range in aqueous medium; however, sidechain pK_a values can change substantially within proteins, vitiating a straightforward conclusion that a histidine group(s) participates directly in the transition.

That the time course of phase 2 varies with the position of the caged residue agrees well with the idea that mutations at various positions result in distinct conformations of the receptor. After the flash, however, all mutants produce the same wild-type receptor, and thus very likely the same open conformation. Therefore, these experiments provide good evidence for a concept often discussed but not proven: point mutations can affect gating of ion channels by changing the structure of the closed state(s) in addition to the directly measurable effects on the open state(s).

The relative contribution of phase 1 increases during a flash series. The mechanism for this increase should be studied in further experiments with increased temporal resolution and varying conditions. The use of time-resolved electrophysiology with sidechain decaging appears to be a promising technique, because it has revealed a range of phenomena inviting further study.

Experimental Procedures

Chemical Synthesis

The α-amino group of the aminoacylated tRNA was protected by 4PO (Madsen et al., 1995) until just before injection into oocytes (see below). 4PO–Tyr(ONB)–tRNA was prepared from 4PO–Tyr(ONB) cyanomethyl ester following established procedures (Nowak et al., 1998). The cyanomethyl ester was synthesized from L-tyrosine in several steps, as detailed below (Silverman, 1998).

Cu(L-Tyr)$_2$ was prepared by mixing L-tyrosine with three equivalents of NaOH and 0.5 equivalents of $CuSO_4$ in water at 60°C for 10 min, quenching with acetic acid, and then filtering. To a solution of 400 mg Cu(L-Tyr)$_2$ and 261 mg K_2CO_3 in 16 ml 75% aqueous DMF was added 357 mg nitrobenzyl chloride. The mixture was stirred for 2 days, providing a cloudy light-blue mixture which was suction-filtered, and the precipitate was rinsed with 75% aqueous DMF, water, and acetone. The resulting solid was stirred with 10 ml 1 N HCl for 1 hr and then filtered and rinsed with 1 N HCl, water, and acetone, providing 130 mg of Tyr(ONB) as an off-white solid. FAB-MS MH^+, 317; HRMS calculated for $C_{16}H_{17}N_2O_5$, 317.1137; found, 317.1130.

The Tyr(ONB) was converted to 4PO–Tyr(ONB) cyanomethyl ester in two steps. Tyr(ONB) (130 mg) was mixed with 1.4 equivalents of Na_2CO_3 and dissolved in 6 ml water plus 3 ml dioxane. A solution of 1.4 equivalents 4-pentanoic anhydride in 3 ml dioxane was added; the clear, colorless solution was stirred for 1 hr and then quenched with 25 ml each CH_2Cl_2 and 1 N $NaHSO_4$. The aqueous layer was extracted with 3 × 10 ml CH_2Cl_2, and the organic layers were combined, dried (Na_2SO_4), and filtered. The residue was chromatographed (CH_2Cl_2 to ethyl acetate), providing 59 mg (36%) of 4PO–Tyr(ONB) as a white solid. ^{1}H NMR (CD_3CN) δ 8.07 (dd, J = 8.2, 1.0 Hz, 1H), 7.79 (d, J = 7.6 Hz, 1H), 7.68 (td, J = 7.6, 1.0 Hz, 1H), 7.51 (td, J = 7.7, 1.1 Hz, 1H), 7.12 (d, J = 8.6 Hz, 2H), 6.88 (d, J = 8.6 Hz, 2H), 6.73 (d, J = 7.8 Hz, 1H), 5.72 (m, 1H), 5.38 (s, 2H), 4.94 (m, 2H), 4.59 (m, 1H), 3.08 (dd, J = 14.1, 5.2 Hz, 1H), 2.88 (dd, J = 14.1, 8.1 Hz, 1H), 2.21 (s, 4H). ^{13}C NMR δ 173.46, 173.01, 157.71, 148.05, 137.85, 134.57, 133.84, 131.15, 130.31, 129.56, 129.37, 125.48, 115.49, 115.27, 67.32, 54.15, 36.75, 35.46, 29.93. DCI-MS MH^+ 399 (24), 264 (29), 106 (100). HRMS calculated for $C_{21}H_{23}N_2O_6$, 399.1556; found, 399.1554.

To a solution of 58 mg 4PO–Tyr(ONB) in 1 ml each DMF and chloroacetonitrile was added 62 μl triethylamine (three equivalents). The solution was stirred for 5 hr, and the volatiles were removed under vacuum. The product was chromatographed (CH_2Cl_2 to 9:1 CH_2Cl_2:ethyl acetate), providing 57 mg (88%) of 4PO–Tyr(ONB) cyanomethyl ester as a white solid. ^{1}H NMR (CD_3CN) δ 8.09 (d, J = 8.2 Hz, 1H), 7.79 (d, J = 7.7 Hz, 1H), 7.71 (t, J = 7.6 Hz, 1H), 7.54 (t, J = 7.7 Hz, 1H), 7.14 (d, J = 8.6 Hz, 2H), 6.92 (d, J = 8.6 Hz, 2H), 6.78 (d, J = 7.6 Hz, 1H), 5.74 (m, 1H), 5.42 (s, 2H), 4.95 (m, 2H), 4.74 (s, 2H), 4.61 (m, 1H), 3.06 (dd, J = 14.0, 5.7 Hz, 1H), 2.90 (dd, J = 14.0, 8.7 Hz, 1H), 2.22 (s, 4H). DCI-MS MH^+ 438 (16), 303 (25), 246 (26), 107 (100). HRMS calculated for $C_{23}H_{24}N_3O_6$, 438.1665; found, 438.1666. After chemical ligation to dCA (Nowak et al., 1998), ESI-MS $[M–H]^-$, 1015; calculated for $C_{40}H_{46}N_{10}O_{12}P_2$, 1016.

Unnatural Amino Acid Mutagenesis and Oocyte Injection

The Y93TAG and Y198TAG mutants and the pAMV-PA vector have been described (Nowak et al., 1995); polymerase chain reaction mutagenesis was used to generate a cassette containing the α-Y127TAG amber mutation. The cassette was trimmed with the appropriate restriction enzymes, purified, and ligated into the parent construct (α/pAMV-PA), which had been previously digested with the same restriction enzymes and dephosphorylated.

Synthesis of tRNA followed established procedures (Nowak et al., 1998). The 4PO–Tyr(ONB)–tRNA was deprotected just prior to injection as follows (England et al., 1997). To a room temperature solution of 4PO–Tyr(ONB)–tRNA (0.5 μl) was added a saturated solution of iodine (0.5 μl, 1.2 mM). After 30 min, the resulting Tyr(ONB)–tRNA was immediately mixed with the desired mRNA and microinjected into oocytes. Tyr(ONB) reagents and injected oocytes were handled under lights filtered to block UV.

Optics

A capacitor bank (2600 μf) charged to 450 V was connected to a xenon short-arc flashlamp in a mirrored housing (Nargeot et al., 1982). The rising phase of the flash lasted 0.2 ms, and the time constant of the decay phase was 1 ms. The light was passed through a Schott UG11 filter to provide 300–350 nm and was focused with a 50 mm quartz lens (Oriel) onto a liquid light guide 1 m long and 3 mm in diameter (Oriel 77554); at the chamber, the end of the light guide touched the bottom surface of a horizontal Pyrex coverslip (quartz would have passed more light). The oocyte was placed on this coverslip. A concave first-surface mirror (Rolyn, 20 mm focal length, 50 mm diameter) was placed ~40 mm above the oocyte and positioned for maximal intensity. (For a diagram of the apparatus, see http://www.neuron.org/supplemental/20/4/619.)

Electrophysiology

Whole-cell currents from oocytes were measured using a Gene Clamp 500 amplifier (Axon Instruments) in the two-electrode voltage-clamp configuration. To attain optimal time resolution, we used agarose cushion electrodes with resistances between 0.2 and 0.6 MΩ (Schreibmayer et al., 1994). Grounding and shielding arrangements reduced artifactual flash-induced current transients to <2 ms for oocytes expressing wild-type nAChR and exposed to ACh. To eliminate transients further for the traces in Figure 4, we subtracted traces from flashes after the ACh was washed from the chamber. The holding potential was −80 mV. Oocytes were continuously perfused with a nominally calcium-free bath solution consisting of 96 mM NaCl, 2 mM KCl, 1 mM $MgCl_2$, 5 mM HEPES (pH 7.5), and 1 μM atropine. Relaxation kinetics were analyzed using CLAMPFIT from pCLAMP 6.0 (Axon Instruments).

Acknowledgments

This work was supported by grants from the National Institutes of Health (NS-11756, NS-34407). We thank Mark W. Nowak, Patrick C. Kearney, and Rory Sayres for help and Justin Gallivan for continuing

advice. J. C. M. held Caltech undergraduate research fellowships; P. M. E. held an NRSA.

Received December 17, 1997; revised February 9, 1998.

References

Adams, P.R. (1981). Acetylcholine receptor kinetics. J. Membr. Biol. *58*, 161–174.

Cook, S.N., Jack, W.E., Xiong, X., Danley, L.E., Ellman, J.A., Schultz, P.G., and Noren, C.J. (1995). Photochemically initiated protein splicing. Angew. Chem. Int. Ed. Engl. *34*, 1629–1630.

England, P.M., Lester, H.A., Davidson, N., and Dougherty, D.A. (1997). Site-specific, photochemical proteolysis applied to ion channels in vivo. Proc. Natl. Acad. Sci. USA *94*, 11025–11030.

Figl, A., Labarca, C., Davidson, N., Lester, H.A., and Cohen, B.N. (1996). Voltage-jump relaxation kinetics for wild-type and chimeric β subunits of neuronal nicotinic receptors. J. Gen. Physiol. *107*, 369–379.

Galzi, J.-L., and Changeux, J.-P. (1995). Neuronal nicotinic receptors: molecular organization and regulations. Neuropharmacology *34*, 563–582.

Gurney, A.M., and Lester, H.A. (1987). Light-flash physiology with synthetic photosensitive compounds. Physiol. Rev. *67*, 583–617.

Karlin, A., and Akabas, M.H. (1995). Toward a structural basis for the function of nicotinic acetylcholine receptors and their cousins. Neuron *15*, 1231–1244.

Lester, H.A., and Nerbonne, J.M. (1982). Physiological and pharmacological manipulations with light flashes. Ann. Rev. Biophys. Bioeng. *11*, 151–175.

Madsen, R., Roberts, C., and Fraser-Reid, B. (1995). The pent-4-enoyl group: a novel amine-protecting group that is readily cleaved under mild conditions. J. Org. Chem. *60*, 7920–7926.

McCray, J.A., and Trentham, D.R. (1989). Properties and uses of photoreactive caged compounds. Annu. Rev. Biophys. Biophys. Chem. *18*, 239–270.

Mendel, D., Ellman, J.A., and Schultz, P.G. (1991). Construction of a light-activated protein by unnatural amino acid mutagenesis. J. Am. Chem. Soc. *113*, 2758–2760.

Nargeot, J., Lester, H.A., Birdsall, N.J.M., Stockton, J., Wassermann, N.H., and Erlanger, B.F. (1982). A photoisomerizable muscarinic antagonist. Studies of binding and of conductance relaxations in frog heart. J. Gen. Physiol. *79*, 657–678.

Nerbonne, J.M. (1996). Caged compounds: tools for illuminating neuronal responses and connections. Curr. Opin. Neurobiol. *6*, 379–386.

Nowak, M.W., Kearney, P.C., Sampson, J.R., Saks, M.E., Labarca, C.G., Silverman, S.K., Zhong, W., Thorson, J., Abelson, J.N., Davidson, N., et al. (1995). Nicotinic receptor binding site probed with unnatural amino acid incorporation in intact cells. Science *268*, 439–441.

Nowak, M.W., Gallivan, J.P., Silverman, S.K., Labarca, C.G., Dougherty, D.A., and Lester, H.A. (1998). *In vivo* incorporation of unnatural amino acids into ion channels in a *Xenopus* oocyte expression system. Methods Enzymol., in press.

Saks, M.E., Sampson, J.R., Nowak, M.W., Kearney, P.C., Du, F., Abelson, J.N., Lester, H.A., and Dougherty, D.A. (1996). An engineered *Tetrahymena* tRNAGln for *in vivo* incorporation of unnatural amino acids into proteins by nonsense suppression. J. Biol. Chem. *271*, 23169–23175.

Schreibmayer, W., Lester, H.A., and Dascal, N. (1994). Voltage clamp of *Xenopus laevis* oocytes utilizing agarose-cushion electrodes. Pflügers Arch. *426*, 453–458.

Silverman, S.K. (1998). I. Conformational and charge effects on high-spin organic polyradicals. II. Studies on the chemical-scale origin of ion selectivity in potassium channels. PhD thesis, California Institute of Technology, Pasadena, CA.

Tatsu, Y., Shigeri, Y., Sogabe, S., Yumoto, N., and Yoshikawa, S. (1996). Solid-phase synthesis of caged peptides using tyrosine modified with a photocleavable protecting group: application to the synthesis of caged neuropeptide Y. Biochem. Biophys. Res. Commun. *227*, 688–693.

Wieboldt, R., Ramesh, D., Carpenter, B.K., and Hess, G.P. (1994). Synthesis and photochemistry of photolabile derivatives of γ-aminobutyric acid for chemical kinetic investigations of the γ-aminobutyric acid receptor in the millisecond time region. Biochemistry *33*, 1526–1533.